Enzymatic Characterization and Comparison of Various Poaceae UDP-GlcA 4-Epimerase Isoforms

Xiaogang Gu[1,2], Christopher J. Wages[2], Kathryn E. Davis[2], Paul J. Guyett[2] and Maor Bar-Peled[1,2,*]

[1]*Department of Plant Biology; and* [2]*Complex Carbohydrate Research Center, University of Georgia, Athens, GA 30602-4712, USA*

UDP-α-D-galacturonic acid (UDP-GalA) is a key precursor for the synthesis of various bacterial and plant polysaccharides. UDP-glucuronic acid 4-epimerase (UGlcAE) catalyses the reversible conversion of UDP-α-D-glucuronic acid to UDP-GalA. UGlcAEs isolated from bacterial species have different biochemical properties when compared with the isoenzymes from the plant dicot species, *Arabidopsis*. However, little is known about the specificity of UGlcAE in Poaceae species. Therefore, we cloned and expressed in *Escherichia coli* several maize and rice UGlcAE genes, and compared their enzymatic properties with dicot homologs from *Arabidopsis*. Our data show that UGlcAE isoforms in different plant species have different enzymatic properties. For example, the Poaceae UGlcAE enzymes from rice and maize have significantly lower K_i for UDP-xylose when compared with the *Arabidopsis* enzymes. The epimerases from different plant species are very specific and unlike their bacterial homolog in *Klebsiella pneumoniae*, can only use UDP-GlcA or UDP-GalA as their substrate. This study demonstrates that although members of the plant UGlcAE isoforms are highly conserved, the *in vitro* enzymatic activity of specific Poaceae isoform(s) may be regulated differently by specific nucleotide or nucleotide sugar.

Key words: *Arabidopsis thaliana*, GalA containing glycans, isoform, Poaceae, UDP-glucuronic acid 4-epimerase.

Abbreviations: UGlcAE, UDP-GlcA 4-epimerase; UDP-Xyl, UDP-xylose; UDP-Glc, UDP-glucose; UDP-Gal, UDP-galactose; UDP-Ara, UDP-arabinose.

D-Galacturonic acid (GalA) is a sugar residue found in distinct bacterial polysaccharides and in various plant glycans. GalA is a component of capsular polysaccharides and lipopolysaccharides of several bacterial species (*1–3*). In plants, all pectic polymers: homogalacturonan, rhamnogalacturonan I, rhamnogalacturonan II, xylogalacturonan and apiogalacturonan, contain GalA residue in their backbones (*4*). GalA is also present in the reducing end-sequence of the spruce and *Arabidopsis* xylans (*5, 6*) and in the arabinogalactan protein (*7, 8*). UDP-α-D-galacturonic acid (UDP-GalA), the activated nucleotide sugar form of GalA, has been demonstrated to be the precursor for the synthesis of several GalA containing polysaccharides in bacteria (*2, 9*) and for the synthesis of pectin in plants (*10*). It has been suggested that at least four different galacturonosyltransferases are required to transfer the GalA from UDP-GalA during the synthesis of the plant pectic polymers (*10, 11*).

In bacteria, genes encoding UDP-glucuronic acid 4-epimerase (UGlcAE) have been isolated from type I *Streptococcus pneumoniae* (Cap1J, *2*) and *Klebsiella pneumoniae* (Gla$_{KP}$, *3*) and biochemical data indicate that these two different bacterial UGlcAEs have distinct biochemical properties. For example, in addition to the reversible conversion of UDP-GlcA and UDP-GalA, Gla$_{KP}$ is capable of reversibly interconverting UDP-glucose/UDP-galactose and UDP-*N*-acetylglucosamine/UDP-*N*-acetylgalactosamine (*3*). Cap1J, on the other hand, is specific for UDP-uronic acids (*2*). In plant, a UGlcAE gene family containing six isoforms has been identified in *Arabidopsis* (*12*); each isoform is predicted to have a type-II membrane protein topology and some have been functionally characterized (*12–14*). However, little is known about the specificity of UGlcAEs in Poaceae species (*e.g.* maize and rice) and no Poaceae UGlcAE homologs have been identified or characterized so far. Therefore, to expand our knowledge of Poaceae UGlcAE isoforms, we identified, cloned and characterized the UGlcAE homologs in maize and rice, and subsequently compared their enzymatic properties with the *Arabidopsis* homologs.

MATERIALS AND METHODS

Cloning and Expression Analysis of Arabidopsis, Maize and Rice UGlcAEs—Maize (*Zea mays*) expressed sequence tag cDNA databases (dbEST) were searched to identify cDNAs that encode amino acid sequences similar to the *A. thaliana* UDP-GlcA 4-epimerase1 (AtUGlcAE1). Several expressed sequence tags

---

*To whom correspondence should be addressed.
Tel: 706-542-4496, Fax: 706-542-4412,
E-mail: peled@ccrc.uga.edu

(CO519975, CA830134, BQ668208, BU050741) that showed similarity to the AtUGlcAEl gene products were identified and used to design primers to isolate the corresponding cDNA. Total RNA from seedlings of *Zea mays* ecotype B73 was isolated using Trizol reagent (Gibco-BRL, Gaithersburg, MD, USA), and was reverse transcribed into cDNA as described (*12*). An aliquot (4 µl) of the resulting reverse-transcribed products was used as a template for PCR using 1 U of high-fidelity Platinum Taq DNA polymerase (Invitrogen, Carlsbad, CA, USA), 0.2 µM of the sense primer [ZmCO519975Bsp1S#1 5′-GT CATGAGGGTGTTGGAGGAGGACCTCTTC], 0.2 µM of the anti-sense primer [ZmAY105703Xho1AS#1 5′ CTCG AGTCATTGTCGCGAGTTCTTGGATCC], and 0.2 mM of each dNTP (Roche, Basel) in buffer containing 60 mM Tris–SO$_4$ (pH 8.9), 18 mM ammonium sulphate, 1 mM MgSO$_4$, 5% dimethyl sulfoxide and 1 M betaine. The RT-PCR product (1,332 bp) was separated by agarose-gel electrophoresis, purified and cloned into pCR2.1-TOPO plasmid (Invitrogen). The resulting vector pCR2.1:Zm#1 was sequenced and the nucleotide sequence corresponding to the maize gene was submitted to GenBank (accession no. DQ247999, ZmUGlcAE3). The truncated version of ZmUGlcAE3 gene, which lacks the portion encoding the putative transmembrane domain (Δ1–47), was subsequently amplified by PCR and cloned into an *Escherichia coli* expression vector as described below. Using pCR2.1:Zm#1 as a template, the PCR was carried out with sense ZmCO519975Nde1S#2 5′-CATATGACGGCGTCCTACCTCAGCTTCCAGTC and anti-sense ZmAY105703HindIII AS#2 5′-AAGCTTTCAT TGTCGCGAGTTCTTGGATCC primers, and high-fidelity Platinum Taq DNA polymerase as above. After 20-PCR cycles, the DNA product (1,191 bp) was isolated from agarose-gel and cloned into pCR4-TOPO plasmid (Invitrogen) to generate pCR4:Zmt#14. After DNA sequencing, the Nde I-Hind III fragment from pCR4:Zmt#14, consisting of the coding region spanning from amino acid 48–440 of ZmUGlcAE3 (*i.e.* ZmUGlcAE3$_{\Delta 1-47}$), was subcloned into the Nde I/Hind III cloning sites of pET30a *E. coli* expression vector (Novagen, Madison, WI, USA) resulting in clone pET30a:Zmt#14.2.

For the cloning of the *Arabidopsis* and rice UGlcAE homologues, total RNA was extracted from *Arabidopsis thaliana* ecotype Columbia plants or from seedlings of *Oryza sativa japonica* cultivar-group Sariceltik and the corresponding homologues were obtained by RT-PCR as described above. For the expression of the *Arabidopsis* homologues (AtUGlcAE2, At3g23820; AtUGlcAE3, At4g30440) and rice UGlcAE homologues (OsUGlcAE1, GenBank DQ333338; OsUGlcAE2, GenBank DQ333337; OsUGlcAE3, GenBank DQ333336) in *E. coli*, the truncated coding regions lacking the putative transmembrane regions (Δ1–68 for AtUGlcAE2, Δ1–53 for AtUGlcAE3, Δ1–72 for OsUGlcAE1, Δ1–68 for OsUGlcAE2 and Δ1–53 for OsUGlcAE3) were amplified by PCR reactions using the corresponding cDNAs as templates and with the following primers: sense BAB03000#3S 5′-CATA TGCACCACCTCCACCGTCGTAGCTTCTTATC and anti-sense BAB03000#2AS 5′-GCGGCCGCTTAAGCGGA ATCTTCGGCGTGAG for AtUGlcAE2; sense 188BspH1trunS#4 5′-CTCATGAGCTTCGTCGATTCCGG

TAG and anti-sense 188kpn1bamh1AS#3 5′-GGATCCGG TACCATATGTACAAGCTTGGCTTTAG for AtUGlcAE3; sense R20Nco1S#2 5′-CCATGGCCCCGCGGGCGGCGCC CGACTC and anti-sense R20BamH1AS#1 5′-GGATCCC TTGCACTGCTTGTGTTGCCACTCCG for OsUGlcAE1; sense R10BspH1S#2 5′-TCATGAGCCACTCCTTCCACCT CTCCTCCG and anti-sense R10BamH1AS#1 5′-GGATCC GACGCGGCGGACATGGCCATGG for OsUGlcAE2; sense R30BspH1S#2 5′-CTCATGAGCTTCCAGTCCTTCGTCGA CACCTC and anti-sense R30BamH1AS#1 5′-GGATCCAA GTTCTTGGAGCCCCTGGTGTAGCC for OsUGlcAE3. The corresponding PCR products were subcloned into pCR2.1-TOPO plasmid or pCR4-TOPO plasmid to gener- ate pCR2.1:63, pCR4:188.2, pCR4:R20tc.3, pCR4:R10t.1 and pCR4:R30t.3, respectively. Upon confirmation of each plasmid construct by DNA sequencing, the Nde I–Not I fragment from pCR2.1:63, the BspH I–BamH I fragment from pCR4:188.2, the BspH I–BamH 1 fragment from pCR4:R10t.1, the Nco I–BamH I fragment from pCR4:R20tc.3 and the BspH I–BamH I fragment from pCR4:R30t.3 were subcloned into Nde I/Not I or Nco I/ BamH I cloning sites of the pET28b *E. coli* expression vector (Novagen, Madison, WI, USA) resulting in clones pET28b:63.5AC, pET28b:188.1, pET28b:R10t.3, pET28b: R20t.1 and pET28b:R30t.9, respectively.

For ZmUGlcAE3 expression studies, total RNA was isolated from 8 cm long ears, the 10th leaf (from the bottom) or from the roots and whole seedling of 1-week- old maize plants (ecotype w23). RNA (3 µg) was reverse transcribed as described (*12*), and one-twentieth of each of the reverse-transcribed products was used as a tem- plate for PCR using 0.5 U Taq DNA polymerase (Roche), the manufacturer's buffer, 0.2 mM dNTP, 1.5 mM MgCl$_2$, 5% dimethyl sulfoxide, 1 M betaine and 0.2 mM ZmUGlcAE3 gene-specific sense and anti-sense primers (see above). The transcript of ubiquitin (*15*) was used as internal RT-PCR control. PCR conditions were: 1 cycle at 94°C for 3 min; and 30 cycles (94°C, 30 s; 62°C, 30 s; 70°C, 2.5 min) and a final extension at 70°C for 5 min. Twenty more cycles were performed for leaf samples to yield enough products to check the ZmUGlcAE3/ubiquitin expressions. One-tenth of each sample and the DNA MW marker (1 KB plus; Invitrogen) were resolved on a Tris–acetate EDTA-1% agarose gel and visualized by staining with ethidium bromide.

Protein Expression, Purification and Mass Determination—Cultures of *E. coli* carrying the pET30a:Zmt#14.2 (ZmUGlcAE3$_{\Delta 1-47}$), pET28b:63.5AC (AtUGlcAE2$_{\Delta 1-68}$), pET28b:188.1 (AtUGlcAE3$_{\Delta 1-53}$), pET28b:R20t.1 (OsUGlcAE1$_{\Delta 1-72}$), pET28b:R10t.3 (OsUGlcAE2$_{\Delta 1-68}$), pET28b:R30t.9 (OsUGlcAE3$_{\Delta 1-53}$) or control empty vector, were used to inoculate 0.5 l Luria–Bertani liquid broth supplemented with 50 µg/ml kanamycin and 30 µg/ml chloramphenicol. Cell growth, induction and protein isolation were as described (*12*). For unknown reasons, the expression of recombinant OsUGlcAE1$_{\Delta 1-72}$ and OsUGlcAE2$_{\Delta 1-68}$ in *E. coli* were unsuccessful. Estimation of the molecular weight of the native recombinant proteins were carried out on a gel- filtration column (1 cm × 90 cm, packed with Superdex75 prep grade; Amersham Bioscience, Piscataway, NJ, USA) as described (*12*). The active fractions of the recombinant

proteins were further fractionated on an anion-exchange column (0.5 cm × 5 cm, packed with Source Q15; Pharmacia, Piscataway NJ, USA) (*12*). Proteins were separated by 0.1% SDS–12% PAGE (*16*) alongside molecular weight markers (BioRad) and visualized by Coomassie blue staining (Invitrogen).

Enzyme Assay, HPLC and NMR Product Analysis—The typical UDP-GlcAE assay was carried out in a total volume of 50 μl consisting of 0.1 M sodium phosphate (pH 7.6), 20% (v/v) glycerol, 1 mM UDP-GlcA and 1 μg/ml recombinant epimerase. The assay was carried out for 30 min at 37°C (unless otherwise indicated), and the reaction was terminated by the addition of 50 μl of chloroform. Assay products were fractionated by SAX-HPLC (*12*) and the peak corresponding to the standard UDP-GalA (eluted at 22.9 min) was collected, lyophilized, resuspended in D_2O and analysed by ^1H-NMR as described below. Proton NMR spectroscopy of reaction product isolated by HPLC was performed at 25°C on a Varian (Palo Alto, CA, USA) Inova spectrometer operating at 500 MHz. The chemical shifts (δ) are reported in p.p.m. relative to external acetone (2.224 p.p.m.).

Real-time NMR reactions (180 μl) were performed at 37°C in 90% D_2O mixtures containing 0.1 M sodium phosphate pH 7.6, 1 mM UDP-GlcA, 0.1% (v/v) glycerol and recombinant $ZmUGlcAE3_{\Delta1-47}$ (1 μg/ml). ^1H NMR spectra were obtained using a Varian Inova 600 MHz spectrometer equipped with a cryogenic probe. Data acquisition was not started until ~5 min after adding the enzyme to the reaction mixture due to spectrometer setup requirements (shimming). Sequential 1D proton spectra were acquired over the course of the enzymatic reaction.

RESULTS

Isolating and Cloning UGlcAE from Maize—The amino acid sequence of AtUGlcAE1 (*12*) was used to identify candidate gene homologs from maize expressed sequence tag database (dbEST) projects and available genomic data. Based on the sequence data, we cloned one putative maize UGlcAE (ZmUGlcAE) cDNA encoding a protein that shares 66% amino acid sequence identity to AtUGlcAE1. The maize UGlcAE has the conserved nucleotide sugar 4-epimerase catalytic motifs, which include the GxxGxxG (x = any amino acid) motif within the N-terminal domain that is likely to be involved in the binding of β-NAD^+, and a catalytic triad consisting of S/T and YxxxK (*12*, *17*). Reverse transcription RT-PCR was performed to determine the tissue-specific expression of the maize cDNA. Transcripts were detected in root, seedling, ear and mature leaf (Fig. 1).

To determine if the maize homologue functions as a UGlcAE, we expressed the gene in *E. coli* and studied its biochemical properties.

ZmUGlcAE Encodes Active UGlcAE—Since we were unable to express recombinant proteins that contain transmembrane domains in *E. coli* (*12*, *18*), the recombinant $ZmUGlcAE_{\Delta1-47}$, lacking the putative transmembrane domain, was expressed in *E. coli* (Fig. 2A, lane 2). The recombinant $ZmUGlcAE_{\Delta1-47}$ converted
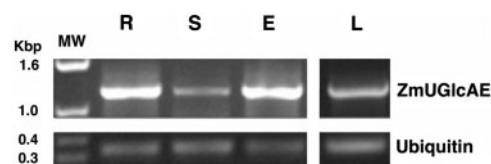

Fig. 1. **ZmUGlcAE transcript is expressed in different maize tissues.** Total RNA isolated from the maize root (R), seedling (S), ear (E) and leaf (L) was used for RT-PCR with gene-specific primers. RT-PCR with ubiquitin specific primers was carried out as an internal control.

UDP-GlcA to UDP-GalA (Fig. 2B, panel 2) while control *E. coli* cells containing empty vector (Fig. 2A, lane 3) had no UGlcAE activity (Fig. 2B, panel 3). $ZmUGlcAE_{\Delta1-47}$ was stable (>6 months) when stored as a crude extract at −20°C, similar to the AtUGlcAE1 (*12*), which is still fully active after 1 year in storage.

To further characterize the protein, the recombinant $ZmUGlcAE_{\Delta1-47}$ was purified by chromatography (Fig. 2A, lane 4). The purified 42.9 kDa $ZmUGlcAE_{\Delta1-47}$ converts UDP-GlcA to a product that elutes from the HPLC column at a retention time of 22.9 min (Fig. 2B, panel 5), with the same elution time as the UDP-GalA standard (Fig. 3, panel 1). To characterize the enzymatic product, the peak eluting from the column at 22.9 min was collected and analysed by ^1H-NMR. The proton chemical shifts and coupling constants data obtained from the 500-mHz ^1H-NMR spectrum of the enzymatic product (data not shown) are identical to those obtained from authentic UDP-GalA (*12*) confirming that $ZmUGlcAE_{\Delta1-47}$ converts UDP-GlcA to UDP-GalA. The data shown in Fig. 3 also demonstrate that $ZmUGlcAE_{\Delta1-47}$ is a 4-epimerase capable of converting UDP-GalA to UDP-GlcA. Like the *Arabidopsis* isoform, the maize UGlcAE does not require exogenous NAD^+ for activity (Fig. 3, panels 3 and 6).

Time-course NMR-based enzyme assay is a powerful method used to monitor reactions without termination and to detect all intermediates and unstable products (*19*). We set to monitor the UGlcAE activity of $ZmUGlcAE_{\Delta1-47}$ by ^1H-NMR. The time-course assay (Fig. 4) clearly showed that UDP-GalA peaks between 3.5 and 4.5 p.p.m. (Fig. 4A, corresponding to α-D-GalA H-2″, H-3″, H-4″ and H-5″ protons), and peaks at 5.66 p.p.m. (Fig. 4B, corresponding to the H-1″ proton of α-D-GalA) are increasing in size while peaks corresponding to protons of UDP-α-D-GlcA are reduced (Fig. 4A and B). Further analyses of the recombinant maize $ZmUGlcAE_{\Delta1-47}$ demonstrated that the enzyme is specific for UDP-uronic acids and cannot use other nucleotide sugars such as UDP-Glc, UDP-Gal, UDP-Xyl, UDP-Ara, as substrates (data not shown).

Enzymatic Characterization of $ZmUGlcAE_{\Delta1-47}$—The optimal pH for the activity of recombinant $ZmUGlcAE_{\Delta1-47}$ is 7.2–7.8 in phosphate buffer, and the optimal temperature is 37°C (Table 1). The activity of $ZmUGlcAE_{\Delta1-47}$ is completely abolished when assays were conducted at pH value <4 or >10, or when the assay temperature was >65°C.
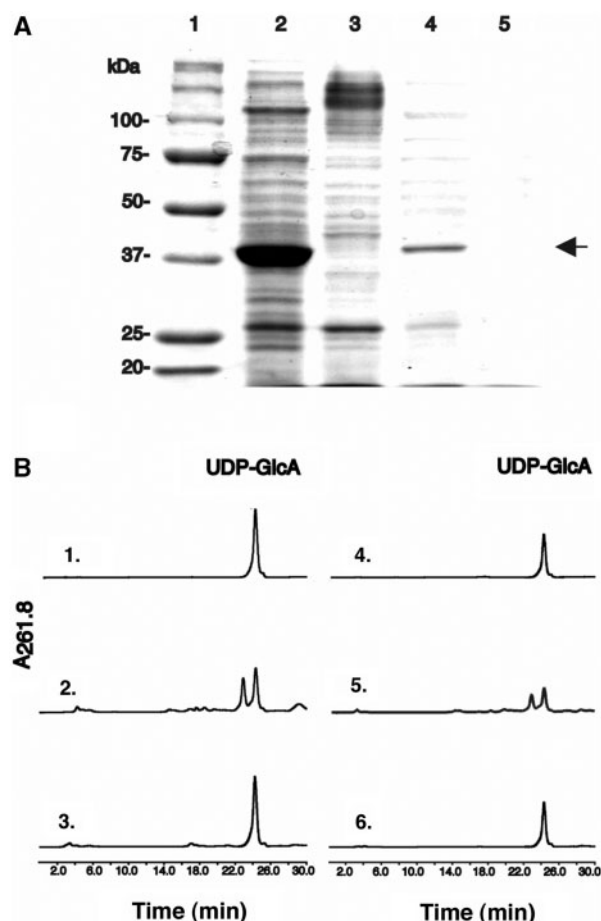
Fig. 2. **Isolation, chromatography and initial characterization of recombinant ZmUGlcAE$_{\Delta 1-47}$.** (A) SDS–PAGE of total protein isolated from *E. coli* cells expressing ZmUGlcAE$_{\Delta 1-47}$ (lane 2) or vector control (lane 3). Proteins from cells expressing recombinant ZmUGlcAE$_{\Delta 1-47}$ were separated by successive chromatographies (see 'MATERIALS AND METHODS' section) and the active fraction eluted from a SourceQ column was separated by SDS–PAGE (lane 4). As a control, total proteins from *E.coli* cells expressing vector alone were separated under the same chromatographic conditions and the corresponding elution fraction from the SourceQ column were separated by SDS–PAGE as well (lane 5). The arrow indicates the position of recombinant ZmUGlcAE$_{\Delta 1-47}$. (B) An aliquot of each protein sample (total protein or protein fraction eluted from SourceQ column) was incubated with UDP-GlcA and the enzymatic reactions were separated on ion exchange HPLC column. The migration of UDP-GlcA standard is indicated in panels 1 and 4. Activity of total protein isolated from cells expressing recombinant ZmUGlcAE$_{\Delta 1-47}$ (panel 2) or vector alone (panel 3) was determined using 1 mM UDP-GlcA as substrate. The activity of column-purified protein isolated from cells expressing recombinant ZmUGlcAE$_{\Delta 1-47}$ (panel 5), or control vector alone that was fractionated on the same SourceQ column (panel 6), was determined using 0.5 mM UDP-GlcA as substrate.

The equilibrium constant (UDP-GalA/UDP-GlcA) is 1.9 (Table 1). Further kinetic analyses indicate that the ZmUGlcAE$_{\Delta 1-47}$ has an apparent K_m value of 396.5 µM for UDP-GlcA and a turnover number (k_{cat}) of 10.1/s. The catalytic efficiency [k_{cat}/K_m] value of the maize UGlcAE is 25.5/mM/s (Table 1). Thus the enzymatic characteristics
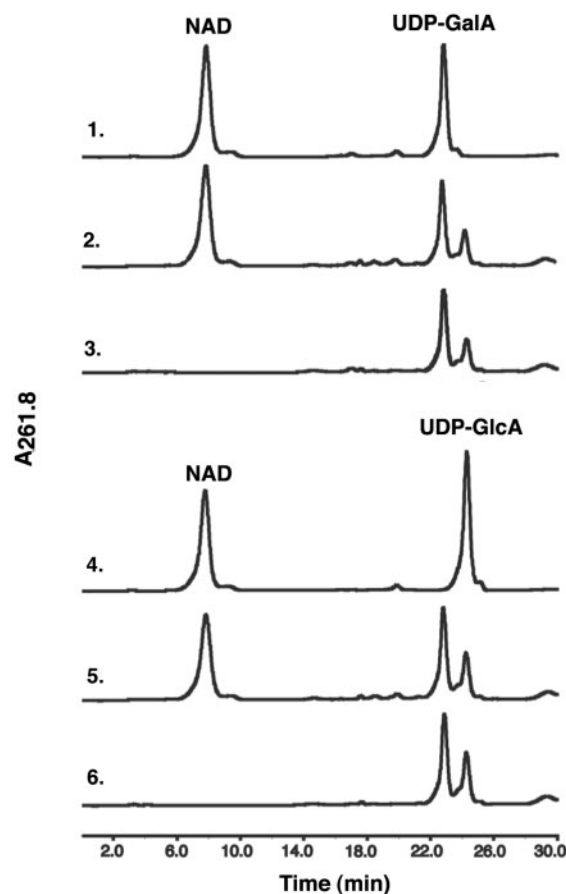
Fig. 3. **Recombinant ZmUGlcAE$_{\Delta 1-47}$ is a reversible UDP-GlcA/UDP-GalAE, and does not require exogenous NAD⁺.** HPLC separation of NAD⁺, UDP-GalA and UDP-GlcA standards (panels 1 and 4) and of UGlcAE reaction mixture (panels 2, 3, 5 and 6). Recombinant ZmUGlcAE$_{\Delta 1-47}$ was incubated for 2 h with 1 mM UDP-GalA and 1 mM NAD⁺ (panel 2), with 1 mM UDP-GalA but without NAD⁺ (panel 3), 1 mM UDP-GlcA and 1 mM NAD⁺ (panel 5) or with 1 mM UDP-GlcA but without NAD⁺ (panel 6).

of ZmUGlcAE$_{\Delta 1-47}$ are comparable with those of *Arabidopsis* AtUGlcAE1$_{\Delta 1-64}$ (*12*).

To determine the apparent molecular weight (M_r) of the active ZmUGlcAE$_{\Delta 1-47}$, the recombinant enzyme was analysed by size-exclusion chromatography on a Superdex75 column. ZmUGlcAE$_{\Delta 1-47}$ activity was detected at an elution volume corresponding to a mass of ∼82 kDa (Table 1), suggesting that the recombinant maize enzyme is active as a dimer *in vitro* assays, similar to the prokaryotic Cap1J (*2*) and *Arabidopsis* AtUGlcAE1 (*12*) enzymes.

UDP-Xyl and UDP Strongly Inhibit the Activity of ZmUGlcAE$_{\Delta 1-47}$—The activity of ZmUGlcAE$_{\Delta 1-47}$ was tested in the presence of different nucleotides and nucleotide sugars and compared with that of *Arabidopsis* isoform AtUGlcAE1 (Fig. 5). The activities of ZmUGlcAE$_{\Delta 1-47}$ and AtUGlcAE1$_{\Delta 1-64}$ were inhibited by 2 mM UDP and UDP-Xyl, but not by 2 mM UMP, GDP or GMP (Fig. 5). Similar to AtUGlcAE1$_{\Delta 1-64}$,
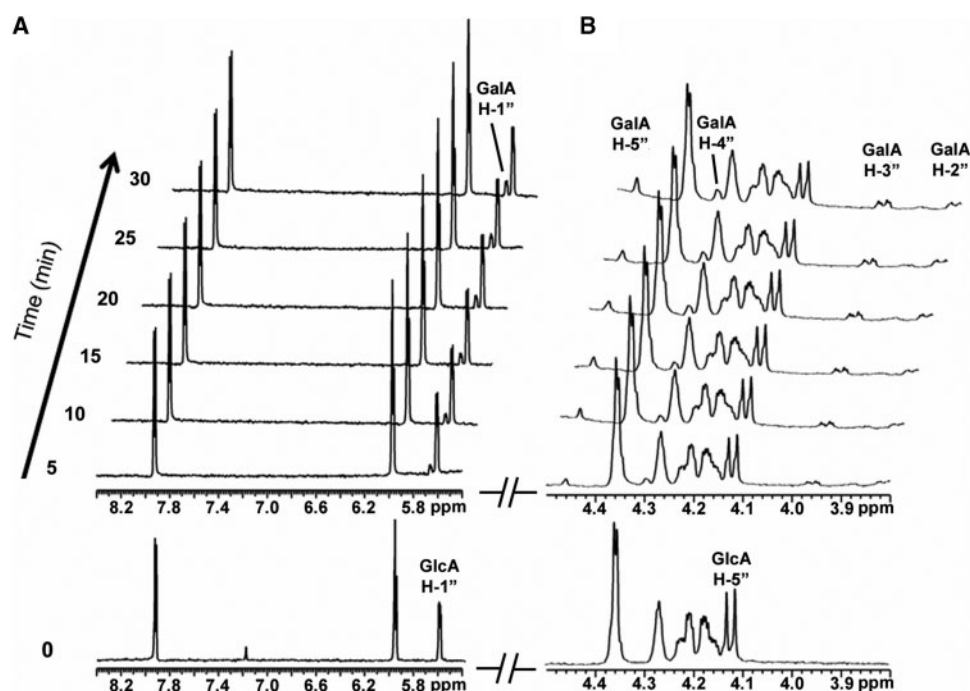
Fig. 4. **Real-time ^{1}H-NMR analysis of the product generated by reacting UDP-GlcA with recombinant ZmUGlcAE$_{\Delta 1-47}$.** The NMR based-assays were carried out at 37°C, in the 600 mHz spectrometer, and representatives of the total 180 spectra collected over the reaction period are shown. (A) A portion of the ^{1}H-NMR observed time resolved spectra (5.5–5.8 p.p.m.) showing the increasing of the UDP-GalA anomeric proton as UGlcAE converts UDP-GlcA to UDP-GalA. (B) A portion of spectra between 3.8 and 4.5 p.p.m. formation showing the increasing of the peaks belonging to the carbon ring protons of UDP-GalA during the time course. Abbreviations of labelled peaks corresponding to the specific sugar protons are: GalA H-1″ (anomeric proton of UDP-GalA), GalA H-2″ (H-2″ proton of UDP-GalA), GalA H-3″ (H-3″ proton of UDP-GalA), GalA H-4″ (H-4″ proton of UDP-GalA), GalA H-5″ (H-5″ proton of UDP-GalA), GlcA H-1″ (anomeric proton of UDP-GlcA) and GlcA H-5″ (H-5″ proton of UDP-GlcA).

Table 1. **Enzymatic characterization of recombinant ZmUGlcAE$_{\Delta 1-47}$, OsUGlcAE3$_{\Delta 1-53}$, AtUGlcAE3$_{\Delta 1-53}$ and AtUGlcAE2$_{\Delta 1-68}$.**

	Optimal pH[a]	Optimal temperature[b] (°C)	K_m[c] (μM)	k_{cat} (S^{-1})	Catalytic efficiency (mM^{-1}S^{-1})	Equilibrium constant[d]	Mass of active protein[e] (Denatured) (kDa)
ZmUGlcAE$_{\Delta 1-47}$	7.2–7.8	30–37	396.5 ± 41.8	10.1 ± 2.0	25.5 ± 2.9	1.9 ± 0.1	81.4 (42.9)
OsUGlcAE3$_{\Delta 1-53}$	7.6	37	258.5 ± 7.5	37.4 ± 5.1	144.3 ± 16.4	1.6 ± 0.1	92.2 (44.3)
AtUGlcAE3$_{\Delta 1-53}$	7.6	37	426.3 ± 53.7	10.0 ± 0.8	23.8 ± 4.2	1.5 ± 0.1	88.5 (44.1)
AtUGlcAE2$_{\Delta 1-68}$	7.6	37	358.4 ± 80.8	0.9 ± 0.1	2.5 ± 0.6	0.6 ± 0.1	88.5 (45.5)

[a]Assays were conducted for 30 min in 0.1 M sodium phosphate at various pH values, ranging from 2 to 11.5. [b]Optimal temperature assays were conducted in phosphate buffer (pH 7.6) for 30 min at temperature ranging from 4°C to 65°C. [c]For kinetic studies, assays at different concentrations of UDP-GlcA (0.08–3 mM) were performed for 5 min. The reciprocal initial velocity was plotted against the reciprocal UDP-GlcA concentration according to Lineweaver and Burk to calculate K_m value. [d]Assays were conducted in phosphate buffer (pH 7.6) for different time (0, 10, 20, 30, 90, 300 and 480 min). [e]The molecular mass of the active ZmUGlcAE$_{\Delta 1-47}$, OsUGlcAE3$_{\Delta 1-53}$, AtUGlcAE3$_{\Delta 1-53}$ and AtUGlcAE2$_{\Delta 1-68}$ eluted from a Superdex75 gel filtration column was estimated based on extrapolation of the elution time of standard protein markers.

ZmUGlcAE$_{\Delta 1-47}$ is also not significantly inhibited by 2 mM UDP-Glc or UDP-Gal.

The K_i values of UDP-Xyl (Table 2) for maize ZmUGlcAE$_{\Delta 1-47}$ was significantly lower ($K_i = 73.1$ μM) when compared with the *Arabidopsis* AtUGlcAE1$_{\Delta 1-64}$ (297.2 μM). Similarly, the maize enzyme displayed a much stronger inhibition to UDP ($K_i = 63.2$ μM) than AtUGlcAE1$_{\Delta 1-64}$ ($K_i = 143.6$ μM). We therefore wondered if such distinct inhibition by UDP and UDP-Xyl is specific to Poaceae UGlcAEs, which differentiate them from the dicot enzymes. We thus decided to clone the rice

UGlcAE genes, and further characterized and compared their enzymatic properties with other *Arabidopsis* UGlcAEs.

Comparing the Enzymatic Properties of UGlcAEs in Rice, Maize and Arabidopsis and the Effects of UDP-Xyl and UDP on These Isozymes—Rice contains five UGlcAE homologues based on the BLAST analyses of genomic and EST database. Phylogenetic analysis was used to compare the amino acid sequences of UGlcAE isoforms from *Arabidopsis*, rice and maize. This analysis separates the UGlcAEs into three
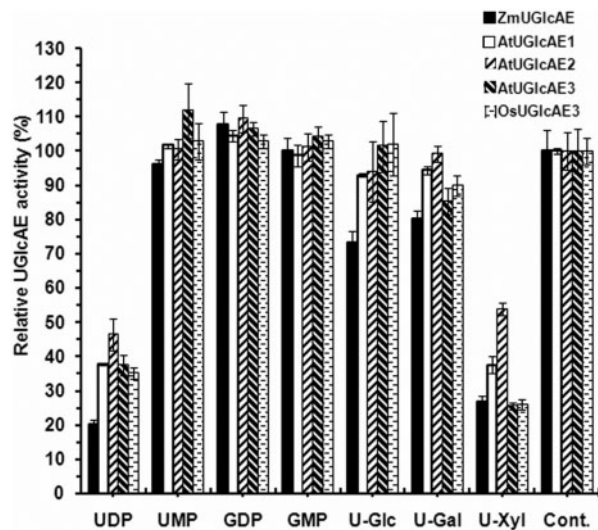
Fig. 5. **The effects of nucleotides and nucleotide sugars on the activity of the recombinant ZmUGlcAE$_{\Delta 1-47}$, AtUGlcAE1$_{\Delta 1-64}$, AtUGlcAE2$_{\Delta 1-68}$, AtUGlcAE3$_{\Delta 1-53}$ and OsUGlcAE3$_{\Delta 1-53}$.** Recombinant ZmUGlcAE$_{\Delta 1-47}$, AtUGlcAE1$_{\Delta 1-64}$, AtUGlcAE2$_{\Delta 1-68}$, AtUGlcAE3$_{\Delta 1-53}$ and OsUGlcAE3$_{\Delta 1-53}$ were first incubated in the absence (control) or presence of different nucleotides and nucleotide sugars (2 mM) for 15 min. Assays were then initiated by adding 1 mM UDP-GlcA and terminated after 30 min. 100% activity corresponds to 700 pmol/min of UDP-GalA produced for ZmUGlcAE$_{\Delta 1-47}$, 970 pmol/min of UDP-GalA produced for AtUGlcAE1$_{\Delta 1-64}$, 463 pmol/min of UDP-GalA produced for AtUGlcAE2$_{\Delta 1-68}$, 624 pmol/min of UDP-GalA produced for AtUGlcAE3$_{\Delta 1-53}$ and 775 pmol/min of UDP-GalA produced for OsUGlcAE3$_{\Delta 1-53}$. The data presented are the average relative amount of UDP-GalA produced compared to the control from three experiments.

Fig. 6. **Neighbour-joining tree of the Maize, Rice and *Arabidopsis* UGlcAE proteins.** UGlcAE protein sequences were aligned with ClustalX software. Alignments were analysed with the PAUP software to generate the unrooted tree. Percentage bootstrap values of 1,000 replicates are given at each branch point. Branch lengths are shown to scale. The Genbank accession number or the loci names are in parentheses: AtUGlcAE1 (At2g45310), AtUGlcAE2 (At3g23820), AtUGlcAE3 (At4g30440), AtUGlcAE4 (At4g00110), AtUGlcAE5 (At1g02000), AtUGlcAE6 (At4g12250), ZmUGlcAE(DQ247999), OsUGlcAE1 (DQ333338), OsUGlcAE2 (DQ333337), OsUGlcAE3 (DQ333336), OsUGlcAE4 (Os09g32670), OsUGlcAE5 (Os06g08810), Cap1J (Z83335).

Table 2. **Inhibition constant (K_i) of U-Xyl and UDP for the recombinant ZmUGlcAE$_{\Delta 1-47}$, OsUGlcAE3$_{\Delta 1-53}$, AtUGlcAE3$_{\Delta 1-53}$, AtUGlcAE2$_{\Delta 1-68}$ and AtUGlcAE1$_{\Delta 1-64}$.**

	$K_{i,\ \text{U-Xyl}}$ (μM)[a]	$K_{i,\ \text{UDP}}$ (μM)[a]
ZmUGlcAE$_{\Delta 1-47}$	73.1 ± 6.9	63.2 ± 14.0
OsUGlcAE3$_{\Delta 1-53}$	159.9 ± 35.3	114.5 ± 20.9
AtUGlcAE3$_{\Delta 1-53}$	274.3 ± 45.5	110.7 ± 16.5
AtUGlcAE2$_{\Delta 1-68}$	305.1 ± 29.4	134.4 ± 8.3
AtUGlcAE1$_{\Delta 1-64}$	297.2 ± 26.9	142.6 ± 4.7

[a]For inhibition constant studies, assays at different concentrations of UDP-GlcA (0.08–3 mM) were performed for 5 min in the presence of 0, 0.1, 0.2 or 0.3 mM inhibitor. The reciprocal initial velocity was plotted against the reciprocal UDP-GlcA concentration to calculate K_i value.

evolutionary clades: Type A, B and C (Fig. 6). Unfortunately, the rice types A and B enzymes were not expressed in *E. coli*, and further analyses were carried out only with the type C rice UGlcAE.

Three more recombinant UGlcAEs (AtUGlcAE2$_{\Delta 1-68}$, AtUGlcAE3$_{\Delta 1-53}$ and OsUGlcAE3$_{\Delta 1-53}$) were expressed and isolated from *E. coli*. The data summarized in Table 1 show that all the recombinant UGlcAEs from different plant species are active as UGlcAE and are active at similar pH range and temperature. Based on
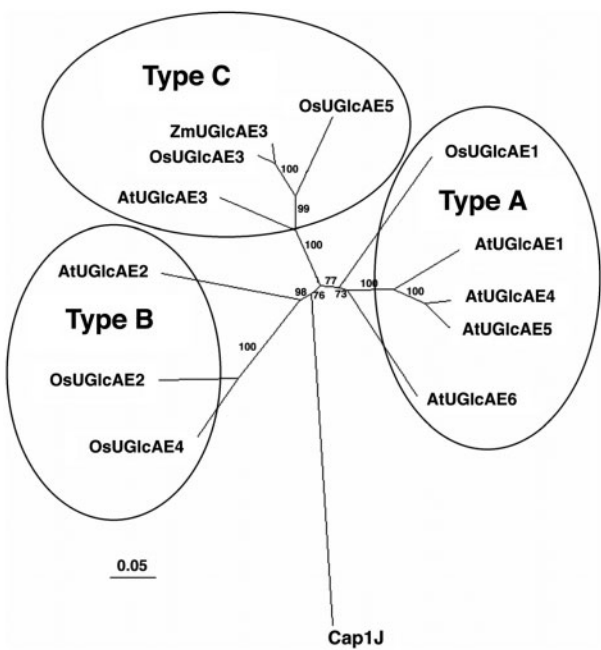
size-exclusion chromatography, all UGlcAE isoforms analysed are active as dimers with the following native molecular masses: AtUGlcAE2$_{\Delta 1-68}$ (88.5 kDa), AtUGlcAE3$_{\Delta 1-53}$ (88.5 kDa) and OsUGlcAE3$_{\Delta 1-53}$ (92.2 kDa). Table 1 also shows that maize, rice and *Arabidopsis* recombinant UGlcAEs have similar K_m values. Except for AtUGlcAE2$_{\Delta 1-68}$, the tested epimerases have comparable k_{cat} and catalytic efficiency kinetic values (Table 1). All five recombinant enzymes are inhibited by 2 mM UDP and UDP-Xyl, but not by 2 mM UMP, GDP, GMP, UDP-Glc or UDP-Gal (Fig. 5). To further compare the catalytic properties of these recombinant enzymes, the effects of UDP and UDP-Xyl (Table 2) on the activities of OsUGlcAE3$_{\Delta 1-53}$, AtUGlcAE2$_{\Delta 1-68}$ and AtUGlcAE3$_{\Delta 1-53}$ were tested and compared at the same time against freshly purified ZmUGlcAE$_{\Delta 1-47}$ and AtUGlcAE1$_{\Delta 1-64}$. Similar to the ZmUGlcAE$_{\Delta 1-47}$, the Poaceae OsUGlcAE3$_{\Delta 1-53}$ have a significantly lower K_i of UDP-Xyl compared with the *Arabidopsis* isoforms (Table 2). Conversely, unlike the ZmUGlcAE$_{\Delta 1-47}$, the *Arabidopsis* isoforms (AtUGlcAE1$_{\Delta 1-64}$, AtUGlcAE2$_{\Delta 1-68}$, AtUGlcAE3$_{\Delta 1-53}$) and OsUGlcAE3$_{\Delta 1-53}$ display a similar inhibition for UDP (Table 2).

DISCUSSION

Our study describes the functional characterization of UGlcAEs in maize and rice and the comparison of their enzymatic properties with the *Arabidopsis* isoforms. In general, all plants whose genomic DNA sequences are available contain multiple UGlcAE isoforms and we established that plant UGlcAEs characterized so far do differ from the bacterial counterparts. For example, the bacterial Cap1J is strongly inhibited by UDP-Gal (*2*) while plant UGlcAEs are not.

Both Poaceae and dicot plants contain pectin as a major component in their cell walls. However, the amount of pectin in Poaceae and dicots is significantly different: <10% in grasses versus ∼30% in dicots; and conversely, grass has a higher content of xylan (20–40%) when compared with dicots (∼5%) (*20*). The biological reason for such differences still remains unclear. It has been suggested that the biosynthesis of cell-wall polysaccharides is controlled by both the glycosyl transferases responsible for assembling the polymers, and by the level of activated nucleotide sugar precursors (*21*, *22*). Therefore, one possible explanation for the relatively lower pectin level in Poaceae when compared with dicots could be that the control of UDP-GalA flux towards pectin synthesis is different between Poaceae and dicots. Our data show that the UGlcAEs from Poaceae (maize ZmUGlcAE3 and rice OsUGlcAE3) have much lower K_i values of UDP-Xyl compared with *Arabidopsis* enzymes (Table 2). A stronger inhibition of Poaceae UGlcAE by UDP-Xyl might lead to the reduction of UDP-GalA level in these plants, resulting in less pectic polymers. Consequently, a relatively higher level of UDP-xylose may be present in Poaceae when compared with *Arabidopsis*, and such differences may explain the higher xylan content in those Poaceae species. On the other hand, however, the regulation of UDP-GalA level by UDP-Xyl could be more complex in plants. For example, numerous studies reported that UDP-Xyl strongly inhibits the activity of the cytosolic enzyme UDP-glucose dehydrogenase (UGDH) (*23–26*). The latter enzyme converts UDP-glucose to UDP-GlcA. Higher levels of UDP-xylose in cytosol will reduce the total UDP-uronic acid made in plants, thus providing another key regulatory step in determining flux of UDP-sugars in the cell. As current experimental methods are unavailable to accurately determine the concentration of UDP-Xyl in the cytosol and Golgi of plant cells, our interpretation of enzyme inhibition by UDP-Xyl is somehow limited until the physiological level of UDP-Xyl becomes available.

A fundamental question in plant biology is why so many isoforms exist for the synthesis of particular metabolites. Several explanations can be proposed: (i) Some isoforms may have different catalytic properties. For example, Barber *et al.* (*27*) who studied isoforms involved in synthesis of UDP-Gal (UDP-glucose 4-epimerase, UGE) demonstrated that the five isoforms display distinct k_{cat} and catalytic efficiency values. Here, we also show that AtUGlcAE3 does display a much less k_{cat} and catalytic efficiency values when it is compared with the other two *Arabidopsis* isoforms. (ii) Different isoforms have evolved to be expressed in a tissue-specific manner. While this may be a case for tobacco sucrose–phosphate synthase isoforms (*28*), the available expression data for the various *Arabidopsis* UGlcAE, UXS and UGE gene family members (*12*, *14*, *18*, *29*) suggest that expression of those isoforms is not tissue specific, although the expression level in specific cell types may be different (*30*). (iii) Some isoforms may be targeted to different locations within a cell or within an organelle. This has been demonstrated for several plant isozymes. For example, of the six UXS isoforms, Uxs1 is localized in Golgi whereas Uxs3 is cytosolic (*31*). Variation of targeting within an organelle was also described for the H_2O_2 scavenging isoenzymes, ascorbate peroxidase (APX). Two distinct types of chloroplastic APXs exist; one is localized in the stroma (sAPX), the other is in the thylakoid (tAPX) (*32*). Clearly, a sub-cellular specific targeting domain is required to target a specific isoform to its final cellular destination. Although the plant UGlcAE isoforms identified so far have a highly conserved catalytic domain, sequence variation does exist, particularly within their N-terminal (approximately first 100 amino acid) and C-terminal (approximately last 25 amino acid) regions. Similar sequence variation at the C and N-termini was observed in the membrane bound UXS isoenzymes (*18*). These specific 'targeting domains' could have evolved, after gene duplication, by inserting the specific nucleotide sequences upstream of the duplicated gene or by fusing an 'intron' to the downstream gene and creating independent targeting sequences over time. We suggest that these distinct 'targeting domains' may localize those isoforms to different endomembranes. Current work in our laboratory is underway to address this possibility.

CONFLICT OF INTEREST

None declared.

REFERENCES

1. Forsberg, L.S. and Carlson, R.W. (1998) The structures of the lipopolysaccharides from *Rhizobium etli* strains CE358 and CE359. *J. Biol. Chem.* **273**, 2747–2757
2. Munoz, R., Lopez, R., de Frutos, M., and Garcia, E. (1999) First molecular characterization of a uridine diphosphate galacturonate 4-epimerase: an enzyme required for capsular

biosynthesis in *Streptococcus pneumoniae* type 1. *Mol. Microbiol.* **31**, 703–713

3. Frirdich, E. and Whitfield, C. (2005) Characterization of Gla$_{KP}$, a UDP-galacturonic acid C4-epimerase from *Klebsiella pneumoniae* with extended substrate specificity. *J. Bacteriol.* **187**, 4104–4115

4. Mohnen, M. (2008) Pectin structure and biosynthesis. *Curr. Opin.Plant Biol.* **11**, 266–277

5. Andersson, S.I. and Samuelson, O. (1983) Structure of the reduced end-groups in spruce xylan. *Carbohyd. Res.* **111**, 283–288

6. Pena, M., Zhong, R., Zhou, G-K., Richardson, E.A., O'Neill, M.A., Darvill, A.G., York, W.S., and Ye, Z.-H. (2007) *Arabidopsis* irregular xylem8 and irregular xylem9: Implications for the complexity of glucuronoxylan biosynthesis. *Plant Cell* **19**, 549–563

7. Clarke, A.E., Anderxn, R.L., and Stone, B.A. (1972) Form and function of arabinogalactans and arabinogalactan-proteins. *Phytochemistry* **18**, 521–540

8. Pellerin, P., Williams, S.V.P., and Brillouet, J.M. (1995) Characterization of five type II arabinogalactan-protein fractions from red wine of increasing uronic acid content. *Carbohyd. Res.* **277**, 135–143

9. Frirdich, E., Bouwman, C., Vinogradov, E., and Whitfield, C. (2005) The role of galacturonic acid in outer membrane stability in *Klebsiella pneumoniae*. *J. Biol. Chem.* **280**, 27604–27612

10. Mohnen, D. (2002) Biosynthesis of pectins in *Pectins and their Manipulation* (Seymour, G.B. and Knox, J.P., eds), pp. 52–98, Blackwell Publishing and CRC Press, Oxford

11. Sterling, J.D., Atmodjo, M.A., Inwood, S.E., Kumar Kolli, V.S., Quigley, H.F., Hahn, M.G., and Mohnen, D. (2006) Functional identification of an *Arabidopsis* pectin biosynthetic homogalacturonan galacturonosyltransferase. *PNAS* **103**, 5236–5241

12. Gu, X. and Bar-Peled, M. (2004) The biosynthesis of UDP-galacturonic acid in plants. Functional cloning and characterization of *Arabidopsis* UDP-D-glucuronic acid 4-epimerase. *Plant Physiol.* **136**, 4256–4264

13. Molhoj, M., Verma, R., and Reiter, W.D. (2004) The biosynthesis of D-Galaturonate in plants, functional cloning and characterization of a membrane-anchored UDP-D-Glucuronate 4-epimerase from *Arabidopsis*. *Plant Physiol.* **135**, 1221–1230

14. Usadel, B., Schluter, U., Molhoj, M., Gipmans, M., Verma, R., Kossmann, J., Reiter, W.D., and Pauly, M. (2004) Identification and characterization of a UDP-D-glucuronate 4-epimerase in *Arabidopsis*. *FEBS Lett.* **569**, 327–331

15. Livak, K.J. and Schmittgen, T.D. (2001) Analysis of relative gene expression data using real-time quantitative PCR and the 2(-Delta Delta C(T)) Method. *Method* **4**, 402–408

16. Bar-Peled, M., Lewinsohn, E., Fluhr, R., and Gressel, J. (1991) UDP-rhamnose:flavanone-7-O-glucoside-2′-O-rhamnosyltransferase, purification and characterization of an enzyme catalyzing the production of bitter compounds in citrus. *J. Biol. Chem.* **266**, 20953–20959

17. Weirenga, R.K., Terpstra, P., and Hol, W.G.J. (1986) Prediction of the occurrence of the ADP-binding beta alpha beta-fold in proteins, using an amino acid sequence fingerprint. *J. Mol. Biol.* **187**, 101–107

18. Harper, A.D. and Bar-Peled, M. (2002) Biosynthesis of UDP-Xylose. Cloning and characterization of a novel *Arabidopsis* gene family, *UXS*, encoding soluble and putative membrane-bound UDP-Glucuronic acid decarboxylase isoforms. *Plant Physiol.* **130**, 2188–2198

19. Guyett, P., Glushka, J., Gu, X., and Bar-Peled, M. (2009) Real-time NMR monitoring of intermediates and labile products of the bifunctional enzyme UDP-apiose/UDP-xylose synthase. *Carbohydr. Res.* In press

20. O'Neill, M. and York, W. (2003) The composition and structure of plant primary cell walls in *The Plant Cell Wall: Annual Plant Review* (Rose, J.K.C., ed.) Vol. 8, pp. 1–54, Blackwell Publishing and CRC Press, Oxford

21. Freshour, G., Bonin, C.P., Reiter, W.D., Albersheim, P., Darvill, A.G., and Hahn, M.G. (2003) Distribution of fucose-containing xyloglucans in cell walls of the *mur1* mutant of *Arabidopsis*. *Plant Physiol.* **131**, 1602–1612

22. Lerouxel, O., Cavalier, M.D., Liepman, H.A., and Keegstra, K. (2006) Biosynthesis of plant cell wall polysaccharides – a complex process. *Curr. Opin. Plant Biol.* **9**, 621–630

23. Davies, M.D. and Dickinson, D.B. (1972) Properties of uridine diphosphoglucose dehydrogenase from pollen of Lilium longiflorum. *Arch. Biochem. Biophys.* **152**, 53–61

24. Campbell, R.E., Sala, R.F., van de Rijn, I., and Tanner, M.E. (1997) Properties and kinetic analysis of UDP-glucose dehydrogenase from group A streptococci. Irreversible inhibition by UDP-chloroacetol. *J. Biol. Chem.* **272**, 3416–3422

25. Turner, W. and Botha, F.C. (2002) Purification and kinetic properties of UDP-glucose dehydrogenase from sugarcane. *Arch. Biochem. Biophys.* **407**, 209–216

26. Bar-Peled, M., Griffith, C.L., Ory, J.J., and Doering, T.L. (2004) Biosynthesis of UDP-GlcA, a key metabolite for capsular polysaccharide synthesis in the pathogenic fungus Cryptococcus neoformans. *Biochem. J.* **381**, 131–136

27. Barber, C., Rösti, J., Rawat, A., Findlay, K., Roberts, K., and Seifert, G. (2006) Distinct properties of the five UDP-D-glucose/UDP-D-galactose 4-epimerase isoforms of *Arabidopsis thaliana*. *J. Biol. Chem.* **281**, 17276–17285

28. Chen, S., Hajirezaei, M., and Bornke, F. (2005) Differential expression of sucrose-phosphate synthase isoenzymes in tobacco reflects their functional specialization during dark-governed starch mobilization in source leaves. *Plant Physiol.* **139**, 1163–1174

29. Zimmermann, P., Hirsch-Hoffmann, M., Hennig, L., and Gruissem, W. (2004) GENEVESTIGATOR. *Arabidopsis* microarray database and analysis toolbox. *Plant Physiol.* **136**, 2621–2632

30. Birnbaum, K., Shasha, D.E., Wang, J.Y., Jung, J.W., Lambert, G.M., Galbraith, D.W., and Benfey, P.N. (2003) A gene expression map of the *Arabidopsis* root. *Science* **302**, 1956–1960

31. Pattathil, S., Harper, A.D., and Bar-Peled, M. (2005) Biosynthesis of UDP-xylose: characterization of membrane-bound At*Uxs2*. *Planta* **211**, 538–548

32. Panchuk, I.I., Zentgraf, U., and Volkov, R.A. (2005) Expression of the Apx gene family during leaf senescence of *Arabidopsis thaliana*. *Planta* **222**, 926–932